

Intruder dominance in the 0_2^+ state of ^{32}Mg studied with a novel technique for in-flight decays

R. Elder^{1,2}, H. Iwasaki^{1,2}, J. Ash^{1,2}, D. Bazin^{1,2}, P. C. Bender^{1,3}, T. Braunroth⁴, B. A. Brown^{1,2}, C. M. Campbell⁵, H. L. Crawford⁵, B. Elman^{1,2}, A. Gade^{1,2}, M. Grinder^{1,2}, N. Kobayashi⁶, B. Longfellow^{1,2}, A. O. Macchiavelli⁵, T. Mijatović^{1,7}, J. Pereira¹, A. Revel¹, D. Rhodes^{1,2}, J. A. Tostevin⁸, and D. Weisshaar¹

¹*National Superconducting Cyclotron Laboratory, Michigan State University, East Lansing, Michigan 48824, USA*

²*Department of Physics and Astronomy, Michigan State University, East Lansing, Michigan 48824, USA*

³*Department of Physics, University of Massachusetts Lowell, Lowell, Massachusetts 01854, USA*

⁴*Institut für Kernphysik, Universität zu Köln, 50937 Köln, Germany*

⁵*Nuclear Science Division, Lawrence Berkeley National Laboratory, Berkeley, California 94720, USA*

⁶*Research Center for Nuclear Physics, Osaka University, Ibaraki, Osaka 567-0047, Japan*

⁷*Ruđer Bošković Institute, HR-10 002 Zagreb, Croatia*

⁸*Department of Physics, University of Surrey, Guildford, Surrey GU2 7XH, United Kingdom*



(Received 25 July 2019; published 4 October 2019)

The development of advanced γ -ray tracking arrays allows for a sensitive new technique to investigate elusive states of exotic nuclei with fast rare-isotope beams. By taking advantage of the excellent energy and position resolution of the Gamma-Ray Energy Tracking In-beam Nuclear Array, we developed a novel technique to identify in-flight isomeric decays of the 0_2^+ state in ^{32}Mg populated in a two-proton removal reaction. We confirm the $0_2^+ \rightarrow 2_1^+$ γ -ray transition of ^{32}Mg and constrain the 0_2^+ decay lifetime, suggesting a large collectivity. The small partial cross section populating the 0_2^+ state in this reaction provides experimental evidence for the reduced occupancy of the normal configuration of the 0_2^+ state, indicating the intruder dominance of this state.

DOI: [10.1103/PhysRevC.100.041301](https://doi.org/10.1103/PhysRevC.100.041301)

The existence of an island of inversion was first postulated to explain the unexpected excess binding for certain neutron-rich isotopes near the canonical $N = 20$ magic number [1–6]. Since then, similar islands of inversion have been proposed at $N = 8, 28, 40$ [7–11], and more recently at 50 [12] where it has been suggested that the nuclear shell structure is dramatically modified, leading to the appearance of deformed nuclei near these magic numbers. The physics mechanisms underlying the structural changes in neutron-rich nuclei have been explored in recent decades, highlighting important aspects of nuclear interactions, such as the tensor and the three-body forces [13–16]. Many low-energy properties in the $N = 20$ island of inversion can be explained by the intruder 2p2h configurations dominating over the normal 0p0h configurations [2,17,18]. However, recent theoretical studies indicated that the intruder 4p4h configurations are also important [14,15], calling into question the simple picture of the structural changes and configuration mixings in the islands of inversion.

In this Rapid Communication, we report on our studies of the lifetime of the 0_2^+ state of ^{32}Mg and the partial cross section to populate the 0_2^+ state in a two-proton removal reaction to examine the configuration mixing near the center of the $N = 20$ island of inversion. The $B(E2; 2_1^+ \rightarrow 0_2^+)$ value from the measured lifetime allows for a comparison of the quadrupole collectivity between the $2_1^+ \rightarrow 0_2^+$ and the $2_1^+ \rightarrow 0_1^+$ transitions. Meanwhile, the two-proton removal cross section from the $^9\text{Be}(^{34}\text{Si}, ^{32}\text{Mg})X$ reaction is sensitive to the overlap between the ^{32}Mg 0_2^+ state and the ^{34}Si 0_1^+ state, the latter being dominated by 0p0h configurations [17,19].

Many other ^{32}Mg properties, such as the excess binding [1], the reduced 2_1^+ energy [6], and the enhanced $B(E2; 2_1^+ \rightarrow 0_1^+)$ value [4,20–24], are consistent with 2p2h configurations dominating the low-energy states. However, the 4p4h configurations appear essential to reproduce the known properties of the long-lived ($\tau > 10$ ns) 0_2^+ state reported at 1058 keV [5]. In agreement with the importance of the 4p4h configurations suggested in recent shell-model studies [14,15], a schematic model consisting of only three configurations, 0p0h, 2p2h, and 4p4h, successfully characterized the 0_2^+ state of ^{32}Mg , including the measured (t, p) reaction cross section [25,26]. This elusive 0_2^+ state has not been observed since the original discovery in 2010 [5], therefore, an independent confirmation of this state and additional lifetime and reaction cross-section information are needed to validate the importance of the 4p4h configurations.

To study the 0_2^+ state of ^{32}Mg , we developed a novel in-beam spectroscopy technique that is now made possible by taking advantage of advanced γ -ray tracking arrays. At relativistic beam velocities, the 0_2^+ state decays over an average range on the order of 1 m past the target. Therefore, in conventional in-beam experiments, the decay location of the 0_2^+ state remains unknown, and the γ -ray energies cannot be corrected for Doppler shift. In our technique, we overcome this difficulty by tracking the isomeric decay position as detailed later in the text. This technique can be applied more generally to in-beam experiments involving isomers with lifetimes on the order of nanoseconds depending on γ -ray yield.

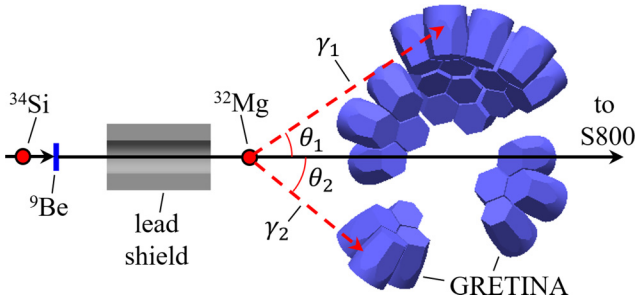


FIG. 1. The present experimental setup. The ${}^9\text{Be}({}^{34}\text{Si}, {}^{32}\text{Mg})X$ reaction populates the 0_2^+ isomer which emits a cascade of γ -rays γ_1 and γ_2 at angles θ_1 and θ_2 relative to the ion trajectory.

This experiment was performed at the NSCL Coupled Cyclotron Facility [27] using a ${}^{48}\text{Ca}$ primary beam at 140 MeV/nucleon on a ${}^9\text{Be}$ production target. A ${}^{34}\text{Si}$ secondary beam at 86 MeV/nucleon was selected by the A1900 fragment separator [28] with a purity of 82% and an intensity of 9×10^5 pps. The 0_2^+ state of ${}^{32}\text{Mg}$ was populated in the ${}^9\text{Be}({}^{34}\text{Si}, {}^{32}\text{Mg})X$ reaction on a 0.57 g/cm^2 -thick ${}^9\text{Be}$ target using the setup shown in Fig. 1. To validate our method, we examined the ${}^{31}\text{Mg}$ products created simultaneously from the same setup which populates a $(7/2^-)$ isomer at 461 keV with a lifetime of $\tau = 15.1(12)$ ns [29]. Reaction products were identified by time-of-flight and energy-loss measurements from the S800 spectrograph [30].

In general, the in-flight detection of isomers with a lifetime from 1 to 100 ns is challenging because decays occur along a flight path on the order of meters. When the isomer produces a cascade of γ rays emitted nearly simultaneously, one solution is to use the timing information of the cascade to locate the common decay position [31]. Our approach is similar, except we use the energy information of the γ -ray cascade, which is now feasible by using the excellent position and energy resolution of the Gamma-Ray Energy Tracking In-beam Nuclear Array (GRETINA) [32]. In practice, if the energy of one observed γ -ray γ_1 is consistent with the Doppler-shifted energy of the known transition, we then assume it is associated with the γ -ray cascade emitted from the isomer. In the ${}^{32}\text{Mg}$ case, the 885-keV transition from the 2_1^+ state has laboratory-frame energy in the range from approximately 610 to 1290 keV. If the observed γ -ray γ_1 is within this energy range, then the Doppler-shift emission angle θ_1 is calculated and used with the hit position of γ_1 in GRETINA to locate the decay position. Then, we can determine the emission angle θ_2 for the other γ -ray γ_2 observed in coincidence. At our ion velocity of $0.353c$, if the lifetime of the 0_2^+ state in ${}^{32}\text{Mg}$ is $\tau \approx 10$ ns, the average flight path is ≈ 1 m. Therefore, to cover the wide range of possible decay positions, the ${}^9\text{Be}$ target was placed 72 cm upstream of the center of GRETINA (Fig. 1). To improve the signal-to-background ratio for detecting isomeric decays, a cylindrical lead shield was installed downstream of the target, attenuating the prompt γ rays from short-lived states, such as the 2_1^+ and 4_1^+ states of ${}^{32}\text{Mg}$. GRETINA was arranged to have four detector modules at 58° , two at 90° , and four at 122° relative to the beam axis measured from

the center of GRETINA. In this arrangement, GRETINA was most efficient for decays occurring 52 to 92 cm downstream of the target, corresponding to ± 20 cm from the center of GRETINA, and we selected events within this range to reduce the background.

The decays we analyzed emit two γ rays in cascade that both may interact with GRETINA multiple times. The highly segmented geometry of GRETINA allows one to distinguish the multiple interaction points, but some criteria must be applied to determine which interaction points belong to each incoming γ ray, and which of those points is the first interaction point within GRETINA. Following the technique used in Ref. [32], the interaction point with the largest energy deposit was chosen as the first interaction point of one γ ray. Then an add-back routine analogous to that used in Ref. [33] was implemented to sum energies within an $r = 80$ -mm sphere centered on the first interaction point. Using the remaining interaction points, a second γ ray was reconstructed with the first interaction point and add-back energy found in the same manner. In general, if interaction points still remain, the same add-back routine can be repeated to define additional γ rays. However, to improve the signal-to-noise ratio, we selected events with exactly two interaction spheres (γ -ray multiplicity two). As mentioned earlier, if one γ -ray γ_1 is assigned to the known transition, then the Doppler-corrected energy of the other γ -ray γ_2 is determined event by event based on the common decay position.

First, we demonstrate the new technique by applying it to the ${}^{31}\text{Mg}$ products as shown in Fig. 2(a) together with a partial level scheme. The spectrum is gated on the 171-keV transition which was used as a reference to determine the decay position of the isomer at 461 keV, allowing the Doppler-shift correction of the coincident 240-keV transition. The peak in Fig. 2(a) was fit with a Gaussian with a centroid energy of 244(5) keV which is consistent with the literature value of 239.9(5) keV. The low energy of the 240-keV γ -ray transition suggests that all its interaction points in GRETINA are likely to occur within an $r = 20$ -mm sphere centered on the first interaction point. Therefore, to improve the sensitivity to events of interest, an additional gate requiring all interaction points of the coincident γ ray to occur within 20 mm of the first interaction point was implemented. Including this gate results in the lower filled spectrum of Fig. 2(a) which shows a reduced background while retaining 66% of the peak counts. The scaled background spectrum in black in Fig. 2 was obtained by analyzing all ${}^{34}\text{Si}$ reaction products excluding the Mg isotopes, which mostly consist of ${}^{34}\text{Si}$ and ${}^{33}\text{Al}$.

The energy spectrum of ${}^{31}\text{Mg}$ was studied further with a GEANT4 simulation [33,34] that included the isomeric 461-keV state, the lower-lying 221- and 50-keV states, and the γ -ray transitions at 240, 221, 171, and 50 keV as shown in the level scheme of Fig. 2(a). The simulated spectrum was added to the background and scaled to fit the measured peak at 244 keV. The simulated energy of the transition from the isomer that best reproduced the data was 239(1) keV as is shown with the red line in Fig. 2(a). The difference between the best-fit energy of 239 keV and the peak centroid energy of 244 keV was attributed to the $\tau = 192$ -ps lifetime of the

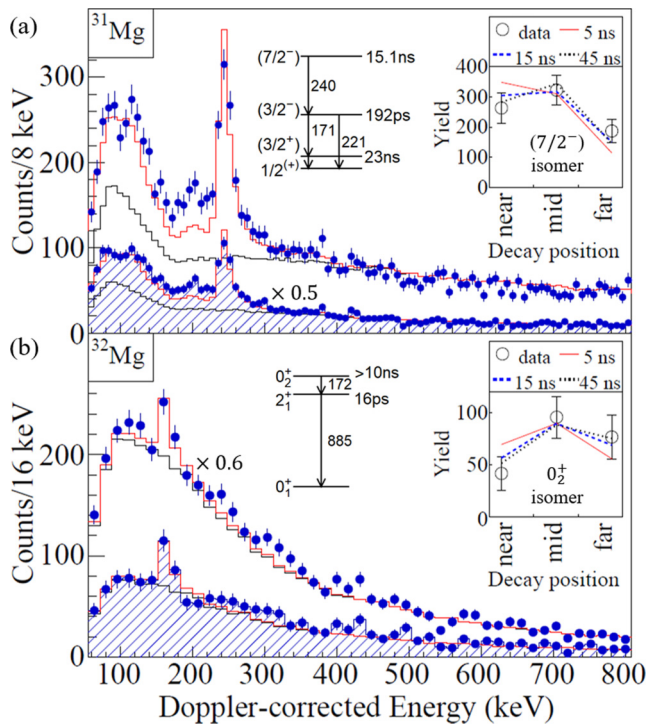


FIG. 2. Doppler-corrected γ -ray energy spectra are shown for data (blue circles), background from the scaled response of beam products excluding the Mg isotopes (black lines), and the sums of the simulated and background responses (red lines). ^{31}Mg is shown (a) in the upper spectra and the constraint that the 244-keV transition only interacts within $r = 20$ mm of its first interaction is included in the lower filled spectrum (scaled by 0.5). ^{32}Mg is shown (b) with the $r = 20$ -mm gate applied to the coincident γ ray in the upper spectrum (scaled by 0.6), and with additional gates requiring proper identification of the interaction points of the 885-keV γ ray in the lower filled spectrum. The insets show the number of decays near (250–525 mm) at middistance (525–700 mm) and far from the target (700–1000 mm). The data (open circles) are compared to simulations assuming lifetimes of 5 ns (red solid line), 15 ns (blue dashed line), and 45 ns (black dotted line).

221-keV state, corresponding to an average distance of 2 cm between the emission points of the 171-keV and the 240-keV γ rays.

The lifetime of the 461-keV state was studied using the distribution of decay positions along the beam line shown in the inset of Fig. 2(a). Although GRETINA is most efficient for decays from 52 to 92 cm downstream of the target, the decay trend was analyzed in a larger region from 25 to 100 cm past the target to improve the sensitivity to the lifetime. The decay distribution does not change significantly for lifetimes greater than 10 ns, so we cannot place an upper limit on the lifetime of the 461-keV state. However, these data place a 1σ lower limit of 9 ns which is consistent with the known lifetime of $\tau = 15.1(12)$ ns [35].

The ^{32}Mg result is shown in Fig. 2(b) where the same analysis approach is used, except now the 885-keV transition from the 2_1^+ state of ^{32}Mg is used as a reference to find the decay location. Since the expected energy of the

$0_2^+ \rightarrow 2_1^+$ transition (172 keV) is low, similar to the 240-keV transition of ^{31}Mg , we used the same condition that all interaction points of the coincident γ ray occur within $r = 20$ mm of the first interaction point. The upper spectrum of Fig. 2(b) shows a peaklike structure close to 170 keV corresponding to the $0_2^+ \rightarrow 2_1^+$ transition [5]. The background distribution is reproduced by analyzing other products of the ^{34}Si beam and scaling the result as shown in black. To understand the significance of the peak at 170 keV, the measured spectrum was compared to a simulation including the 0_2^+ isomer at 1058 keV and the cascade of γ rays with energies 172 and 885 keV. The 2_1^+ state was also included in the simulation using the lifetime value of $\tau = 16(3)$ ps determined from $B(E2)$ results [4,20–24,36]. The simulated distribution was added to the background distribution and scaled to fit the peak at 170 keV as shown by the red line.

The 170-keV peak was unambiguously confirmed by applying additional gates to the 885-keV candidate. The result is shown in Fig. 2(b) as the lower filled spectrum presenting a clear signal with reduced background. In analogy with the $r = 20$ -mm gate applied to the interaction points of the 170-keV transition in ^{32}Mg , a gate was applied that requires all interaction points of the 885-keV γ ray to lie within $r = 60$ mm of the first interaction point. Additionally, we used the interaction point information of the detected 885-keV γ ray to test if it is consistent with Compton scattering. The energies of the first interaction and remaining interactions were used in the Compton scattering formula to obtain the scattering angle (see Eq. (21) of Ref. [37]). If this angle agreed within 0.7 rad with the scattering angle deduced from the decay position and interaction position information, the event passed the gate. In this Rapid Communication, the $0_2^+ \rightarrow 2_1^+$ energy is $165 \pm 4(\text{stat}) \pm 2(\text{syst})$ keV which is included in the simulated response in Fig. 2(b). The 7-keV difference between this measurement and the previous measurement of 172(2) keV [5] is larger than the systematic uncertainty in this measurement due to both the lifetime of the 2_1^+ state (3-ps uncertainty, corresponding to 0.6-keV uncertainty in energy) and the decay location calculation (5-mm uncertainty, corresponding to 2-keV uncertainty in energy). The apparent discrepancy between the observations may be due to the limited statistics of the elusive 0_2^+ γ -ray decay in both studies. We adopt the weighted average of 170(2) keV for the energy of the $0_2^+ \rightarrow 2_1^+$ transition. The distribution of decay positions of the 0_2^+ state places an independent 1σ lower limit on the lifetime of 8 ns, confirming the isomeric nature of this state [5]. The upper limit could not be constrained, however, as shown in the inset of Fig. 2(b).

The correlation between the lifetime and the partial cross section populating the 0_2^+ state (including feeding from unobserved higher-lying states) can be studied from the yield of the 170-keV peak, shown as a gray band in Fig. 3. Since the γ -ray efficiency in this measurement strongly depends on the lifetime, the possible cross section can be constrained for a given lifetime or vice versa. For example, if the assumed lifetime is 5–10 ns, the γ -ray efficiency in this setup is maximized, so the deduced cross section must be minimized. The total error in this result includes 20% statistical uncertainty in the yield of

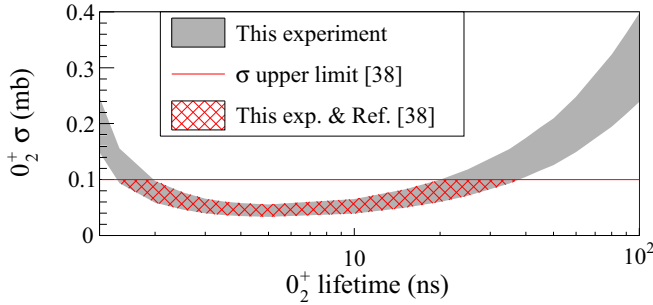


FIG. 3. Possible values for partial cross section and lifetime of the 0_2^+ state of ^{32}Mg within 1σ are plotted (gray band). From the work of Ref. [38], the 1σ upper limit of the cross section at 0.10 mb is included (red line), and the overlap of that work and this Rapid Communication is highlighted (red hatched region).

the 170-keV peak. Another important source of uncertainty is the efficiency of the gates. In order to keep this systematic uncertainty small, the spectrum including fewer gates [Fig. 2(b), upper spectrum] was used in this portion of the analysis and contributes 13% relative uncertainty, estimated by applying the same gates to calibration data taken with a ^{152}Eu source. The statistical and systematic uncertainties were combined in quadrature to a total relative uncertainty of 25% in the cross section at any given lifetime.

The lifetime can be constrained by including the upper limit on the partial cross section of the 0_2^+ state from a previous two-proton removal reaction experiment [38], shown with a red horizontal line in Fig. 3. The previous and present removal reaction experiments populated states in ^{32}Mg using similar midtarget energies of 67 and 75 MeV/nucleon, respectively. Eikonal model calculations based on the two-nucleon amplitudes from the USDB interaction [39] predict 5.11 and 5.23 mb for the inclusive cross section at 67 and 75 MeV/nucleon, respectively, suggesting that the results of the previous removal experiment with a slightly different energy can be safely applied here. In the previous measurement, the 0_2^+ state was not observed, but the 2_1^+ and 4_1^+ states were observed from their γ -ray decays. The measured exclusive cross section populating the 2_1^+ and 4_1^+ states accounted for 100(12)% of the ^{32}Mg inclusive cross section $\sigma_{\text{inc}} = 0.76(10)$ mb. This suggests that, at most, only 12% of the reactions populate the unobserved 0_2^+ state, corresponding to a 1σ upper limit of 0.10 mb for the partial cross section of the 0_2^+ state. With this upper limit in conjunction with the present result, the partial 0_2^+ cross section and lifetime are constrained to $0.03 \text{ mb} < \sigma < 0.10 \text{ mb}$ and $1.5 \text{ ns} < \tau < 38 \text{ ns}$, respectively, as shown by the red hatched region in Fig. 3. The lifetime can be further constrained to $10 \text{ ns} < \tau < 38 \text{ ns}$ from Ref. [5].

Using the 0_2^+ lifetime result of $10 \text{ ns} < \tau < 38 \text{ ns}$ and the weighted average energy of the $0_2^+ \rightarrow 2_1^+$ transition of 170(2) keV, the reduced $E2$ transition probability is $28 \text{ e}^2\text{fm}^4 < B(E2; 2_1^+ \rightarrow 0_2^+) < 122 \text{ e}^2\text{fm}^4$. For physically reasonable values of $\rho^2(E0)$, the $E0$ branch is expected to be less than 1% [5,40]. Therefore, we assumed the $0_2^+ \rightarrow 0_1^+$ transition to be negligible. Table I summarizes the reduced $E2$ transition

TABLE I. $B(E2)$ values of ^{32}Mg and neighboring even-even isotopes.

$B(E2)$ (e^2fm^4)	^{30}Mg	^{34}Si	^{32}Mg
$2_1^+ \rightarrow 0_1^+$	53(7) [41]	17(7) [42]	94(16) [36]
$2_1^+ \rightarrow 0_2^+$	10.9(12) [41]	61(40) [19]	$48_{-20}^{+74\text{a}}$

^aThe central value of $B(E2) = 48 \text{ e}^2 \text{fm}^4$ corresponds to the central lifetime value of 24 ns.

probabilities to 0^+ states in ^{32}Mg and neighboring even-even nuclei which can characterize the quadrupole collectivity in these transitions. For ^{30}Mg , a large $B(E2)$ is observed for the $2_1^+ \rightarrow 0_1^+$ transition [17,43], whereas, in ^{34}Si , a large $B(E2)$ appears for the $2_1^+ \rightarrow 0_2^+$ which suggests a collective nature for the 2_1^+ and 0_2^+ states in ^{34}Si [19]. The present data for ^{32}Mg indicate that the 0_2^+ state is as collective as the 0_1^+ state in contrast with the sizable difference in transition probabilities between 0^+ states in both ^{30}Mg and ^{34}Si . Notably, the $B(E2; 2_1^+ \rightarrow 0_2^+)$ value in ^{32}Mg is comparable to the strong transitions in ^{30}Mg and ^{34}Si and exceeds the values calculated by the three-level mixing model [26] and the SDPF-U-MIX model [19] which both predict $B(E2; 2_1^+ \rightarrow 0_2^+) = 15 \text{ e}^2\text{fm}^4$. The large collectivity in the 0_2^+ state of ^{32}Mg indicates prominent intruder contributions to the state. However, given the large experimental uncertainties, the current $B(E2)$ result does not allow for a stringent conclusion.

Additional direct information about the intruder contributions can be obtained from the partial cross section to populate the 0_2^+ state in comparison with theoretical calculations assuming a pure $0p0h$ configuration. The ^{34}Si 0_1^+ state is predominantly of $0p0h$ configuration [14,17], and the two-proton removal reaction cross section is sensitive to the wave-function overlap between the incoming projectile and the outgoing residual nucleus final state, allowing the $0p0h$ occupancy in the 0_2^+ state of ^{32}Mg to be quantified. Reaction calculations were performed following the method of Ref. [44] which applies the two-neutron amplitudes from shell-model calculations combined with eikonal direct reaction theory. The suppression factor R_{2n} , the ratio of experimental to calculated inclusive two-nucleon removal cross sections, is not known for the (^{34}Si , ^{32}Mg) reaction. We use the value of $R_{2n} = 0.5$ seen for a number of reactions between less-exotic sd -shell beam nuclei and ^9Be targets [44]. The USDB interaction [39] provides an essentially pure $0p0h$ configuration for the ^{32}Mg ground state, and if we assume that it corresponds to the observed 0_2^+ state, then, the 0_2^+ cross section would be $\sigma_{2n} = 0.42 \text{ mb}$. This value is significantly larger than the experimental upper limit of 0.10 mb indicating the physical 0_2^+ state has a reduced $0p0h$ occupancy. The three-level mixing model predicts a smaller $0p0h$ occupancy with a probability $\alpha^2 = 0.15$ for the 0_2^+ state [25] due to the sizable $2p2h$ and $4p4h$ contributions to this state which reduces the overlap with the ^{34}Si 0_1^+ state. By scaling the cross section obtained from the USDB pure $0p0h$ calculation with the $0p0h$ probability α^2 of the 0_2^+ state, the three-level mixing model results in a cross section of 0.06 mb. This result is consistent with the

measured partial cross section, suggesting that the 0_2^+ state contains strong admixtures of the 2p2h and 4p4h intruder configurations.

The present result raises the question, “Where does the 0p0h-dominant 0^+ state exist in ^{32}Mg , if anywhere?” The three-level mixing model predicts the 0_3^+ state at 2.22 MeV with the 0p0h probability $\alpha^2 = 0.81$. This gives the partial cross section $\sigma_{2n} = 0.34$ mb for the 0_3^+ state, although associated events have not been experimentally observed. Using the USDB calculations, the partial cross sections for the individual states are $\sigma(0^+) = 0.42$ mb $\sigma(2^+) = 0.94$ mb, and $\sigma(4^+) = 1.26$ mb for $R_{2n} = 0.50$. The resulting inclusive cross section of 2.62 mb is much larger than the experimental value of 0.76(10) mb [38] as is the case for more exotic nuclei in this mass region [45,46]. This discrepancy indicates either that the R_{2n} is strongly quenched in the (^{34}Si , ^{32}Mg) reaction where the structure is thought to change drastically between the two nuclei or that the 0p0h components in ^{32}Mg are widely spread or even fragmented above the neutron separation energy ($S_n = 5.778$ MeV), calling for future investigation.

In conclusion, a new method to study isomeric states decaying in-flight was used to observe the $0_2^+ \rightarrow 2_1^+$ transition

at 170(2) keV in ^{32}Mg . The $B(E2; 2_1^+ \rightarrow 0_{1,2}^+)$ values of ^{32}Mg reveal that the 0_2^+ state is as collective as the 0_1^+ state, in clear contrast with the neighboring even-even isotopes. From the constrained reaction cross section, it is implied that the 0p0h amplitude in the 0_2^+ state is much reduced by the dominance of intruder configurations. The novel technique introduced here proved indispensable to observe the 0_2^+ state and, as rare-isotope beams with high velocities continue to be powerful tools, this method will prove vital to extend the sensitive lifetime range of in-beam experiments.

This work was supported by the National Science Foundation (NSF) under Grants No. PHY-1565546 and No. PHY-1811855, by the Department of Energy (DOE) National Nuclear Security Administration through the Nuclear Science and Security Consortium under Award No. DE-NA0003180, and by the Science and Technology Facilities (U.K.) Grant No. ST/L005743/1. GREYNA was funded by the DOE, Office of Science. Operation of the array at NSCL was supported by the DOE under Grants No. DE-SC0014537 (NSCL) and No. DE-AC02-05CH11231 (LBNL).

-
- [1] C. Thibault, R. Klapisch, C. Rigaud, A. M. Poskanzer, R. Prieels, L. Lessard, and W. Reisdorf, *Phys. Rev. C* **12**, 644 (1975).
- [2] E. K. Warburton, J. A. Becker, and B. A. Brown, *Phys. Rev. C* **41**, 1147 (1990).
- [3] B. H. Wildenthal and W. Chung, *Phys. Rev. C* **22**, 2260(R) (1980).
- [4] T. Motobayashi, Y. Ikeda, Y. Ando, K. Ieki, M. Inoue, N. Iwasa, T. Kikuchi, M. Kurokawa, S. Moriya, S. Ogawa, H. Murakami, S. Shimoura, Y. Tanagisawa, T. Nakamura, Y. Watanabe, M. Ishihara, T. Teranishi, H. Okuno, and R. F. Casten, *Phys. Lett. B* **346**, 9 (1995).
- [5] K. Wimmer, T. Kröll, R. Krücken, V. Bildstein, R. Gernhäuser, B. Bastin, N. Bree, J. Diriken, P. Van Duppen, M. Huysse, N. Patronis, P. Vermaelen, D. Voulot, J. Van de Walle, F. Wenander, L. M. Fraile, R. Chapman, B. Hadinia, R. Orlandi, J. F. Smith, R. Lutter, P. G. Thirolf, M. Labiche, A. Blazhev, M. Kalkühler, P. Reiter, M. Seidlitz, N. Warr, A. O. Macchiavelli, H. B. Jeppesen, E. Fiori, G. Georgiev, G. Schrieder, S. Das Gupta, G. Lo Bianco, S. Nardelli, J. Butterworth, J. Johansen, and K. Riisager, *Phys. Rev. Lett.* **105**, 252501 (2010).
- [6] C. Détraz, D. Guillemaud, G. Huber, R. Klapisch, M. Langevin, F. Naulin, C. Thibault, L. C. Carraz, and F. Touchard, *Phys. Rev. C* **19**, 164 (1979).
- [7] A. Navin, D. W. Anthony, T. Aumann, T. Baumann, D. Bazin, Y. Blumenfeld, B. A. Brown, T. Glasmacher, P. G. Hansen, R. W. Ibbotson, P. A. Lofy, V. Maddalena, K. Miller, T. Nakamura, B. V. Pritychenko, B. M. Sherrill, E. Spears, M. Steiner, J. A. Tostevin, J. Yurkon, and A. Wagner, *Phys. Rev. Lett.* **85**, 266 (2000).
- [8] B. Bastin, S. Grévy, D. Sohler, O. Sorlin, Zs. Dombrádi, N. L. Achouri, J. C. Angélique, F. Azaiez, D. Baiborodin, R. Borcea, C. Bourgeois, A. Buta, A. Bürger, R. Chapman, J. C. Dalouzy, Z. Dlouhy, A. Drouard, Z. Elekes, S. Franchoo, S. Iacob, B. Laurent, M. Lazar, X. Liang, E. Liénard, J. Mrazek, L. Nalpas, F. Negoita, N. A. Orr, Y. Penionzhkevich, Z. Podolyák, F. Pougheon, P. Roussel-Chomaz, M. G. Saint-Laurent, M. Stanoiu, I. Stefan, F. Nowacki, and A. Poves, *Phys. Rev. Lett.* **99**, 022503 (2007).
- [9] A. Gade, R. V. F. Janssens, T. Baugher, D. Bazin, B. A. Brown, M. P. Carpenter, C. J. Chiara, A. N. Deacon, S. J. Freeman, G. F. Grinyer, C. R. Hoffman, B. P. Kay, F. G. Kondev, T. Lauritsen, S. McDaniel, K. Meierbachtol, A. Ratkiewicz, S. R. Stroberg, K. A. Walsh, D. Weisshaar, R. Winkler, and S. Zhu, *Phys. Rev. C* **81**, 051304(R) (2010).
- [10] B. A. Brown, *Physics* **3**, 104 (2010).
- [11] S. M. Lenzi, F. Nowacki, A. Poves, and K. Sieja, *Phys. Rev. C* **82**, 054301 (2010).
- [12] F. Nowacki, A. Poves, E. Caurier, and B. Bounthong, *Phys. Rev. Lett.* **117**, 272501 (2016).
- [13] O. Sorlin and M.-G. Porquet, *Prog. Part. Nucl. Phys.* **61**, 602 (2008).
- [14] E. Caurier, F. Nowacki, and A. Poves, *Phys. Rev. C* **90**, 014302 (2014).
- [15] N. Tsunoda, T. Otsuka, N. Shimizu, M. Hjorth-Jensen, K. Takayanagi, and T. Suzuki, *Phys. Rev. C* **95**, 021304(R) (2017).
- [16] T. Otsuka, T. Suzuki, J. D. Holt, A. Schwenk, and Y. Akaishi, *Phys. Rev. Lett.* **105**, 032501 (2010).
- [17] Y. Utsuno, T. Otsuka, T. Mizusaki, and M. Honma, *Phys. Rev. C* **60**, 054315 (1999).
- [18] B. A. Brown and B. H. Wildenthal, *Annu. Rev. Nucl. Part. Sci.* **38**, 29 (1988).
- [19] F. Rotaru, F. Negoita, S. Grévy, J. Mrazek, S. Lukyanov, F. Nowacki, A. Poves, O. Sorlin, C. Borcea, R. Borcea, A. Buta, L. Cáceres, S. Calinescu, R. Chevrier, Zs. Dombrádi, J. M. Daugas, D. Lehbertz, Y. Penionzhkevich, C. Petrone, D. Sohler, M. Stanoiu, and J. C. Thomas, *Phys. Rev. Lett.* **109**, 092503 (2012).
- [20] B. V. Pritychenko, T. Glasmacher, P. D. Cottle, M. Fauerback, R. W. Ibbotson, K. W. Kemper, V. Maddalena, A. Navin, R.

- Ronningen, A. Sakharuk, H. Scheit, and V. G. Zelevinsky, *Phys. Lett. B* **461**, 322 (1999).
- [21] V. Chisté, A. Gillibert, A. Leépine-Szily, N. Alamanos, F. Auger, J. Barrette, F. Braga, M. D. Cortina-Gil, Z. Dlouhy, V. Lapoux, M. Lewitowicz, R. Lichtenthäler, R. L. Neto, S. M. Lukyanov, M. MacCormick, F. Marie, W. Mittig, F. de Oliveira Santos, N. A. Orr, A. N. Ostrowski, S. Ottini, A. Pakou, Y. E. Penionzhkevich, P. Roussel-Chomaz, and J. L. Sida, *Phys. Lett. B* **514**, 233 (2001).
- [22] H. Iwasaki, T. Motobayashi, H. Sakurai, K. Yoneda, T. Gomi, N. Aoi, N. Fukuda, Z. Fülöp, U. Futakami, Z. Gacsi, Y. Higurashi, N. Imai, N. Iwasa, T. Kubo, M. Kunibu, M. Kurokawa, Z. Liu, T. Minemura, A. Saito, M. Serata, S. Shimoura, S. Takeuchi, Y. X. Watanabe, K. Yamada, Y. Yanagisawa, and M. Ishihara, *Phys. Lett. B* **522**, 227 (2001).
- [23] J. A. Church, C. M. Campbell, D.-C. Dinca, J. Enders, A. Gade, T. Glasmacher, Z. Hu, R. V. F. Janssens, W. F. Mueller, H. Olliver, B. C. Perry, L. A. Riley, and K. L. Yurkewicz, *Phys. Rev. C* **72**, 054320 (2005).
- [24] K. Li, Y. Ye, T. Motobayashi, H. Scheit, P. Doornenbal, S. Takeuchi, N. Aoi, M. Matsushita, E. Takeshita, D. Pang, and H. Sakurai, *Phys. Rev. C* **92**, 014608 (2015).
- [25] A. O. Macchiavelli, H. L. Crawford, C. M. Campbell, R. M. Clark, M. Cromaz, P. Fallon, M. D. Jones, I. Y. Lee, M. Salathe, B. A. Brown, and A. Poves, *Phys. Rev. C* **94**, 051303(R) (2016).
- [26] A. O. Macchiavelli and H. L. Crawford, *Phys. Scr.* **92**, 064001 (2017).
- [27] B.-M. Sherrill, *Prog. Theor. Phys. Suppl.* **146**, 60 (2002).
- [28] D. J. Morrissey, B. M. Sherrill, M. Steiner, A. Stolz, and I. Wiedenhoever, *Nucl. Instrum. Methods Phys. Res., Sect. B* **204**, 90 (2003).
- [29] H. Nishibata, T. Shimoda, A. Odahara, S. Morimoto, S. Kanaya, A. Yagi, H. Kanaoka, M. R. Pearson, C. D. P. Levy, and M. Kimura, *Phys. Lett. B* **767**, 81 (2017).
- [30] D. Bazin, J. A. Caggiano, B. M. Sherrill, J. Yurkon, and A. Zeller, *Nucl. Instrum. Methods Phys. Res., Sect. B* **204**, 629 (2003).
- [31] S. Shimoura, A. Saito, T. Minemura, Y. U. Matsuyama, H. Baba, H. Akiyoshi, N. Aoi, T. Gomi, Y. Higurashi, K. Ieki, N. Imai, N. Iwasa, H. Iwasaki, S. Kanno, S. Kubono, M. Kunibu, S. Michimasa, T. Motobayashi, T. Nakamura, H. Sakurai, M. Serata, E. Takeshita, S. Takeuchi, T. Teranishi, K. Ue, K. Yamada, Y. Yanagisawa, M. Ishihara, and N. Itagaki, *Phys. Lett. B* **560**, 31 (2003).
- [32] D. Weisshaar, D. Bazin, P. C. Bender, C. M. Campbell, F. Recchia, V. Bader, T. Baugher, J. Belarge, M. P. Carpenter, H. L. Crawford, M. Cromaz, B. Elman, P. Fallon, A. Forney, A. Gade, J. Harker, N. Kobayashi, C. Langer, T. Lauritsen, I. Y. Lee, A. Lemasson, B. Longfellow, E. Lunderberg, A. O. Macchiavelli, K. Miki, S. Momiyama, S. Noji, D. C. Radford, M. Scott, J. Sethi, S. R. Stroberg, Z. Sullivan, R. Titus, A. Wiens, S. Williams, K. Wimmer, and S. Zhu, *Nucl. Instrum. Methods Phys. Res., Sect. A* **847**, 187 (2017).
- [33] C. Loelius, H. Iwasaki, B. A. Brown, M. Honma, V. M. Bader, T. Baugher, D. Bazin, J. S. Berryman, T. Braunroth, C. M. Campbell, A. Dewald, A. Gade, N. Kobayashi, C. Langer, I. Y. Lee, A. Lemasson, E. Lunderberg, C. Morse, F. Recchia, D. Smalley, S. R. Stroberg, R. Wadsworth, C. Walz, D. Weisshaar, A. Westerberg, K. Whitmore, and K. Wimmer, *Phys. Rev. C* **94**, 024340 (2016).
- [34] S. Agostinelli, J. Allison, K. Amako, J. Apostolakis, H. Araujo, P. Arce, M. Asai, D. Axen, S. Banerjee, G. Barrand, F. Behner, L. Bellagamba, J. Boudreau, L. Broglia, A. Brunengo, H. Burkhardt, S. Chauvie, J. Chuma, R. Chytráček, G. Cooperman, G. Cosmo, P. Degtyarenko, A. Dell'Acqua, G. Depaola, D. Dietrich, R. Enami, A. Feliciello, C. Ferguson, H. Fesefeldt, G. Folger, F. Foppiano, A. Forti, S. Garelli, S. Giani, R. Giannitrapani, D. Gibin, J. J. G. Cadenas, I. González, G. G. Abril, G. Greeniaus, W. Greiner, V. Grichine, A. Grossheim, S. Guatelli, P. Gumplinger, R. Hamatsu, K. Hashimoto, H. Hasui, A. Heikkinen, A. Howard, V. Ivanchenko, A. Johnson, F. W. Jones, J. Kallenbach, N. Kanaya, M. Kawabata, Y. Kawabata, M. Kawaguti, S. Kelner, P. Kent, A. Kimura, T. Kodama, R. Kokoulin, M. Kossov, H. Kurashige, E. Lamanna, T. Lampén, V. Lara, V. Lefebvre, F. Lei, M. Liendl, W. Lockman, F. Longo, S. Magni, M. Maire, E. Medernach, K. Minamimoto, P. M. de Freitas, Y. Morita, K. Murakami, M. Nagamatu, R. Nartallo, P. Nieminen, T. Nishimura, K. Ohtsubo, M. Okamura, S. O'Neale, Y. Oohata, K. Paech, J. Perl, A. Pfeiffer, M. G. Pia, F. Ranjard, A. Rybin, S. Sadilov, E. D. Salvo, G. Santin, T. Sasaki, N. Savvas, Y. Sawada, S. Scherer, S. Sei, V. Sirotenko, D. Smith, N. Starkov, H. Stoecker, J. Sulkimo, M. Takahata, S. Tanaka, E. Tcherniaev, E. S. Tehrani, M. Tropeano, P. Truscott, H. Uno, L. Urban, P. Urban, M. Verderi, A. Walkden, W. Wander, H. Weber, J. P. Wellisch, T. Wenaus, D. C. Williams, D. Wright, T. Yamada, H. Yoshida, and D. Zschesche, *Nucl. Instrum. Methods Phys. Res., Sect. A* **506**, 250 (2003).
- [35] The ISOLDE Collaboration, H. Mach, L. M. Fraile, O. Tengblad, R. Boutami, C. Jollet, W. A. Plóciennik, D. T. Yordanov, M. Stanoiu, M. J. G. Borge, P. A. Butler, J. Cedarkäll, P. Fogelberg, H. Fynbo, P. Hoff, A. Jokinen, A. Korgul, U. Köster, W. Kurcewicz, F. Marechal, T. Motobayashi, J. Mrazek, G. Neyens, T. Nilsson, S. Pedersen, A. Poves, B. Rubio, and E. Ruchowska, *Eur. Phys. J. A* **25**, 105 (2005).
- [36] C. Ouellet and B. Singh, *Nucl. Data Sheets* **112**, 2199 (2011).
- [37] T. Lauritsen, A. Korichi, S. Zhu, A. N. Wilson, D. Weisshaar, J. Dudouet, A. D. Ayangeakaa, M. P. Carpenter, C. M. Campbell, E. Clément, H. L. Crawford, M. Cromaz, P. Fallon, J. P. Greene, R. V. F. Janssens, T. L. Khoo, N. Lalović, I. Y. Lee, A. O. Macchiavelli, R. M. Perez-Vidal, S. Pietri, D. C. Radford, D. Ralet, L. A. Riley, D. Seweryniak, and O. Stezowski, *Nucl. Instrum. Methods Phys. Res., Sect. A* **836**, 46 (2016).
- [38] D. Bazin, B. A. Brown, C. M. Campbell, J. A. Church, D. C. Dinca, J. Enders, A. Gade, T. Glasmacher, P. G. Hansen, W. F. Mueller, H. Olliver, B. C. Perry, B. M. Sherrill, J. R. Terry, and J. A. Tostevin, *Phys. Rev. Lett.* **91**, 012501 (2003).
- [39] B. A. Brown and W. A. Richter, *Phys. Rev. C* **74**, 034315 (2006).
- [40] T. Kibédi, T. W. Burrows, M. B. Trzhaskovskaya, P. M. Davidson, and C. W. N. Jr., *Nucl. Instrum. Methods Phys. Res., Sect. A* **589**, 202 (2008).
- [41] M. S. Basunia, *Nucl. Data Sheets* **111**, 2331 (2010).
- [42] R. W. Ibbotson, T. Glasmacher, B. A. Brown, L. Chen, M. J. Chromik, P. D. Cottle, M. Fauerbach, K. W. Kemper, D. J. Morrissey, H. Scheit, and M. Thoennessen, *Phys. Rev. Lett.* **80**, 2081 (1998).
- [43] O. Neidermaier, H. Scheit, V. Bildstein, H. Boie, J. Figging, R. von Hahn, F. Köck, M. Lauer, U. K. Pal, H. Podlech, R. Repnow, D. Schwalm, C. Alvarez, F. Ames, G. Bollen, S. Emhofer, D. Habs, O. Kester, R. Lutter, K. Rudolph, M. Pasini,

- P. G. Thirolf, B. H. Wolf, J. Eberth, G. Gersch, H. Hess, P. Reiter, O. Thelen, N. Warr, D. Weisshaar, F. Aksouh, P. V. den Bergh, P. V. Duppen, M. Huyse, O. Ivanov, P. Mayet, J. V. de Walle, J. Äystö, P. A. Butler, J. Cederkäll, P. Delahaye, H. O. U. Fynbo, L. M. Fraile, O. Forstner, S. Franchoo, U. Köster, T. Nilsson, M. Oinonen, T. Sieber, F. Wenander, M. Pantea, A. Richter, G. Schreider, H. Simon, T. Behrens, R. Gernhäuser, T. Kröll, Krücken, M. Münch, T. Davison, J. Gerl, G. Huber, A. Hurst, J. Iwanicki, B. Jonson, P. Lieb, L. Liljeby, A. Schempp, A. Scherillo, P. Schmidt, and G. Walter, [Phys. Rev. Lett.](#) **94**, 172501 (2005).
- [44] J. A. Tostevin and B. A. Brown, [Phys. Rev. C](#) **74**, 064604 (2006).
- [45] P. Fallon, E. Rodriguez-Vieitez, A. O. Macchiavelli, A. Gade, J. A. Tostevin, P. Adrich, D. Bazin, M. Bowen, C. M. Campbell, R. M. Clark, J. M. Cook, M. Cromaz, D. C. Dinca, T. Glasmacher, I. Y. Lee, S. McDaniel, W. F. Mueller, S. G. Prussin, A. Ratkiewicz, K. Siwek, J. R. Terry, D. Weisshaar, M. Wiedeking, K. Yoneda, B. A. Brown, T. Otsuka, and Y. Utsuno, [Phys. Rev. C](#) **81**, 041302(R) (2010).
- [46] I. Murray, M. MacCormick, D. Bazin, P. Doornenbal, N. Aoi, H. Baba, H. Crawford, P. Fallon, K. Li, J. Lee, M. Matsushita, T. Motobayashi, T. Otsuka, H. Sakurai, H. Scheit, D. Steppenbeck, S. Takeuchi, J. A. Tostevin, N. Tsunoda, Y. Utsuno, H. Wang, and K. Yoneda, [Phys. Rev. C](#) **99**, 011302(R) (2019).